ChemComm

Accepted Manuscript

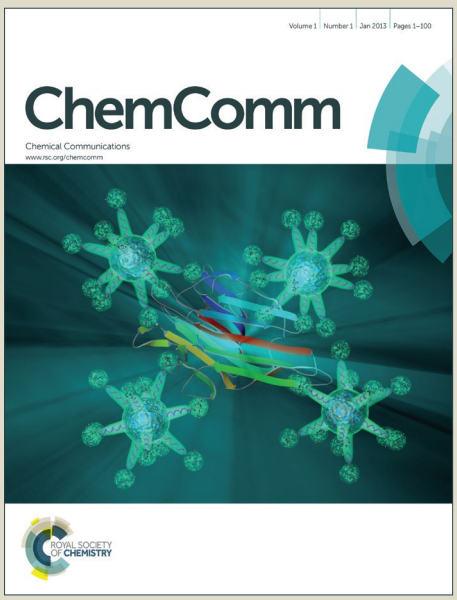

ROYAL SOCIETY OF CHEMISTRY

www.rsc.org/chemcomm

ChemComm

COMMUNICATION

Highly active Pd-P nanoparticles electrocatalyst for enhanced formic acid oxidation synthesized by stepwise electroless deposition

Received 00th January 20xx,
Accepted 00th January 20xx

DOI: 10.1039/x0xx00000x

www.rsc.org/

Kee Chun Poon,[a] Bahareh Khezri[b], Yao Li[a], Richard D. Webster[b], Haibin Su[c] and Hirotaka Sato*[a]

Highly active Pd-P nanoparticles electrocatalyst for formic acid oxidation was synthesized using NaH_2PO_2 as a reducing agent. The Pd-P nanoparticles were amorphous and exhibited higher specific and mass activity values compared to commercial Pd/C electrocatalyts and reported literature values. Furthermore, the Pd-P nanoparticles were found to be more durable than Pd/C electrocatalyts.

Direct formic acid fuel cells (DFAFCs) have attracted much attention as an environmentally-friendly, high performing fuel cell due to their high electromotive force, reduced rate of fuel crossover as well as high power and energy density.[1-5] In particular, palladium (Pd) has received considerable amounts of attention as a replacement for conventional platinum (Pt) due to its lower cost, higher catalytic activity and also its ability to catalyze formic acid oxidation (FAO) through a direct dehydrogenation pathway which makes it less susceptible to CO poisoning.[6-9] However, the major problem with using Pd is that its catalytic activity drops significantly over time.[10-12]

In recent years, many research groups have searched for ways to improve both the catalytic activity and the durability of Pd electrocatalysts.[13-15] Advancements made to improve these properties includes manipulating Pd nanoparticles (NPs) sizes[16-18] or shapes[19-21], combining Pd with other metals to form bimetallic compounds[22-24] as well as altering the morphology of the Pd.[25,26] In particular, manipulating the morphology of Pd to enhance the catalytic activity and durability is still a relatively new research front with many advancement opportunities.[27,28]

Therefore, this work reports a facile synthesis method for highly active Pd-P NPs for enhanced FAO. The Pd-P NPs were shown to be amorphous and had higher specific and mass activity than previously reported in the literature.[24,29,30] Also, these Pd-P NPs were shown to be more stable than commercial Pd/C.

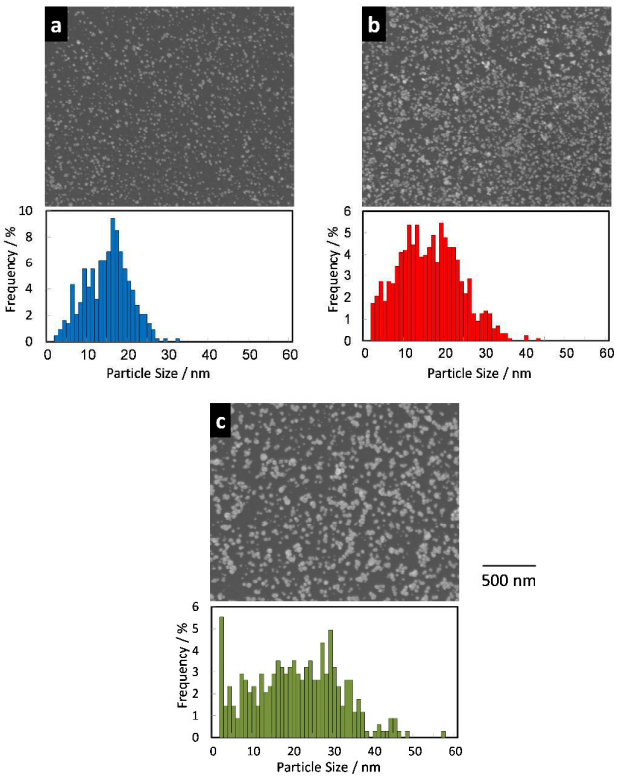

Fig. 1 SEM images (upper) and their corresponding size distribution (lower) of Pd-P for (a) 6 cycles, (b) 9 cycles and (c) 12 cycles of deposition.

[a] *School of Mechanical & Aerospace Engineering, Nanyang Technological University, 50 Nanyang Avenue, Singapore 639798. email:hirosato@ntu.edu.sg*
[b] *Division of Chemistry & Biological Chemistry, School of Physical and Mathematical Sciences, Nanyang Technological University, 21 Nanyang Link, Singapore 637371*
[c] *School of Materials Science & Engineering, Nanyang Technological University, 50 Nanyang Avenue, Singapore 639798*

† Electronic Supplementary Information (ESI) available: Details of experiments and additional characterization results. See DOI: 10.1039/x0xx00000x

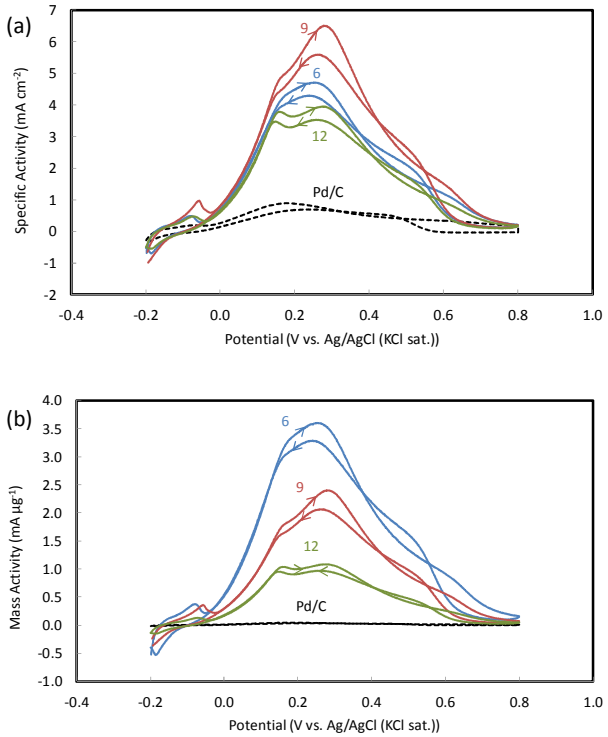

Fig. 2 (a) Specific activity and (b) Mass activity graphs of Pd-P NPs and Pd/C. The number beside the curves denote the number of deposition cycles. The measurements were conducted in N_2-saturated 0.5 M H_2SO_4 + 1 M HCOOH solution. Scan rate: 50 mV s^{-1}.

The Pd-P NPs were prepared by stepwise electroless deposition using $PdCl_2$ and NaH_2PO_2 at room temperature without any harsh conditions or additives as previously reported.[24,31,32] By varying the number of cycles in the electroless deposition method, the electrocatalytic ability of the Pd-P NPs can be tuned accordingly.

The Pd-P NPs were characterized by scanning electron microscopy (SEM). Fig. 1 shows the SEM images of different deposition cycles of Pd-P NPs. Regardless of the number of deposition cycles, the Pd-P NPs were shown to be well dispersed. Also, the mean size of the Pd-P NPs increases with increasing deposition cycles (6, 9 and 12 cycles were 14, 16 and 20 nm respectively). The amorphous nature of the Pd-P NPs were already characterized in a previous work and shown in Fig. S1 (ESI†).[31,33]

The electrocatalytic activities of these Pd-P NPs on FAO were analyzed using cyclic voltammetry (CVs). Fig. 2 shows the CVs conducted in N_2-saturated 0.5 M H_2SO_4 + 1M HCOOH scanned at 50 mV s^{-1}. From Fig. 2, it is indicated by the oxidation peak potentials for FAO occurs in the range of 0 V to 0.3 V. These oxidation peaks occurring within this range verifies that the Pd-P NPs catalyzes the FAO through dehydrogenation pathway which is the preferred pathway.[1,3,24,32] Furthermore, the absence of any oxidation peaks at 0.4 V demonstrates that the undesired indirect oxidation pathway (dehydration pathway) is not present.[3,24,34]

Table 1. Specific, mass activity and average P content values of Pd-P and Pd/C at peak potential

Catalysts	Specific Activity (mA cm^{-2})	Mass Activity (mA μg^{-1})	Average P Content (at%)
6 cyc Pd-P	4.9	2.9	12
9 cyc Pd-P	5.7	2.0	16
12 cyc Pd-P	4.3	1.1	11
Pd/C	0.9	0.05	-

Specific and mass activity values are the averaged results of multiple Pd-P and Pd/C samples.

It is observed in Fig. 2 that there are two discrete peaks in every FAO curve. These two discrete peaks are in agreement with recent studies conducted on the mechanism of FAO.[35-37] It is explained by Joo *et al.* that the first peak at the lower potential (0.17 V) corresponds to $HCOO^-$ being oxidized while the second peak at higher potential (0.28 V) is caused by bridge bonded-adsorbed formate enhancing $HCOO^-$ oxidation at higher potential by preventing the adsorption and oxidation of other species on the electrode surface.[36]

Fig. 2a shows the CVs of different numbers of deposition cycles of Pd-P NPs normalized by electrochemically active surface area (ECSA).[2,7] It conclusively shows that at all the deposition cycles, the specific activities of the Pd-P NPs were higher than the commercial Pd/C. This trend is also observed for the data in Fig. 2b. In Fig. 2b, the CVs of the different cycles of Pd-P NPs were normalized by the amount of Pd loaded onto the GCE instead.[2,7] Again, the mass activities of the Pd-P NPs were shown to be better than the commercial Pd/C at all the varying deposition cycles.

Table 1 summarizes the averaged specific and mass activity values of all the different deposition cycles of the Pd-P NPs as well as the commercial Pd/C. It is reiterated from Table 1 that for both specific as well as mass activity values, amorphous Pd-P NPs outperform the commercial Pd/C at all the deposition cycles. This superior specific and mass activity of the Pd-P NPs is theorized to be the result of the amorphous structure of the Pd-P NPs. Being amorphous in nature, the surface of Pd-P is structurally disordered and contains large numbers of low co-ordination number reactive sites.[28,31] These low co-ordination number reactive sites (edges, defects and kinks) have been reported to increase the catalytic activity towards FAO.[14,28,38-41] Hence, amorphous Pd-P has superior specific and mass activity over commercial Pd/C.

Fig. 3 presents the CVs of the Pd-P NPs deposited on carbon cloth before and after annealing at 700 oc for 1 hour. This annealing temperature and duration are known to change the amorphous Pd to crystalline phase.[42] After the annealing process, the specific activity of the Pd-P drops significantly, which supports the speculation that the amorphous nature of Pd-P is a key factor in its high catalytic activity.

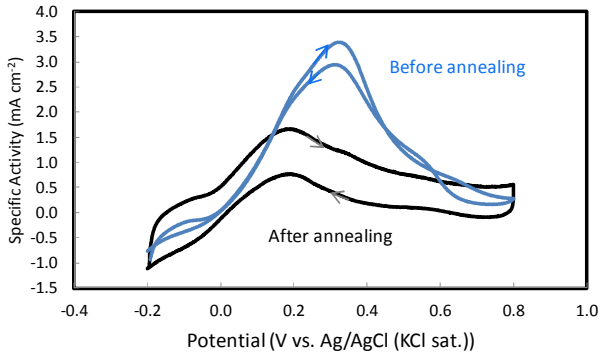

Fig. 3 Specific activity graphs of 6 cycles Pd-P NPs deposited on carbon cloth before and after annealing at 700 °c for 1 hour. The measurements were conducted in N_2-saturated 0.5 M H_2SO_4 + 1 M HCOOH solution. Scan rate: 50 mV s^{-1}.

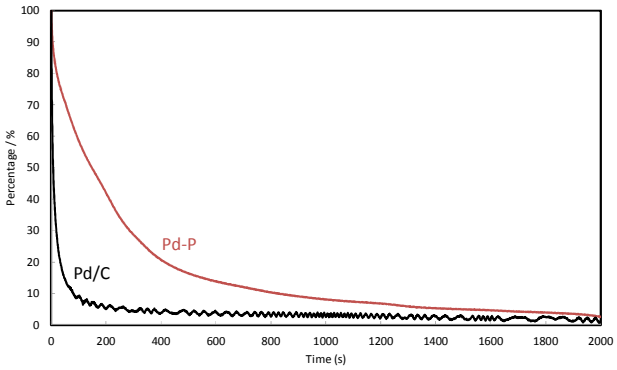

Fig. 4 Chronoamperometry results for Pd-P and Pd/C. Results were evaluated as a percentage of initial current density. The measurements were performed in N_2-saturated 0.5 M H_2SO_4 + 1 M HCOOH solution at 0.2 V vs Ag/AgCl (KCl sat.).

Comparison is made between different deposition cycles of Pd-P for specific activity values. As seen from Table 1, 9 cycles Pd-P had the highest specific activity of 5.7 mA cm^{-2}, followed by 6 cycles Pd-P which had a specific activity of 4.9 mA cm^{-2} and lastly 12 cycles Pd-P which had a specific activity of 4.3 mA cm^{-2}. The highest specific activity (5.7 mA cm^{-2}) is higher than any previously reported values from the literature.[24,30] Also from Table 1, the average P content for 6 cycles Pd-P was 12 at% while 9 cycles Pd-P was 16 at% and 12 cycles Pd-P was 11 at%. This trend is reflective of that observed for the specific activity. It is suggested that, with more P doping, the surface of Pd-P becomes increasingly structurally disordered which results in greater number of low co-ordination active sites.[28,31] These low co-ordination active sites are known to increase catalytic activity.[14,28,38-41] Hence, with greater number of these low co-ordination active sites, the specific activity increases. The reverse would also be true. With less P doping, there would be less low co-ordination active sites and would cause the specific activity to drop. Therefore the trend of the average P content of 6, 9 and 12 cycles Pd-P would explain the trend of the specific activity.

Table 1 also shows a decreasing trend for the mass activity values with increasing deposition cycles. The maximum mass activity value (2.9 mA μg^{-1}) is also higher than any previously reported literature values.[24,29] The decreasing trend would be because of increased probability of coagulation of Pd-P NPs and particle size with increasing deposition cycles (Fig. 1). Increased coagulation and particle size would mean lower mass activity values as less Pd is exposed to the electrolyte (wasted Pd).

Fig. 4 compares the durability of the Pd-P with that of the commercial Pd/C. It is demonstrated that the Pd-P is more durable with respect to Pd/C as seen from the gentle slope of the percentage of the initial current density of Pd-P compared to the sharp slope of Pd/C. The percentage current density of Pd-P at 400, 800 and 1200 s were 21%, 10% and 7% of the initial value while for Pd/C it was 4%, 3% and 2% respectively. This clearly shows that at each corresponding time interval, the drop in percentage current density for Pd-P was always lesser than Pd/C. This conclusively shows that Pd-P is more durable, efficient and has better poisoning resistance compared to Pd/C.

In summary, this report demonstrated a facile stepwise electroless deposition method for synthesizing Pd-P NPs which were characterized to be amorphous. These Pd-P NPs demonstrated higher specific and mass activity values than commercial Pd/C and those previously reported in the literature.[24,29,30] Furthermore, these Pd-P NPs were shown to be more durable than Pd/C. Importantly, this report promotes the potential of amorphous materials as catalysts not solely for fuel cells but also for other catalytic applications.

This work was supported by the Nanyang Assistant Professorship (NAP, M4080740) and Singapore Ministry of Education (MOE2013-T2-2-049). The authors appreciate Ms. Koh Joo Luang, Ms. Yong Mei Yoke and Mr. Leong Kwok Phui, Materials Laboratories at MAE, NTU, for their continuous effort to set up and maintain an excellent experimental environment.

Notes and references

1. E. Antolini, *Energy & Environmental Science*, 2009, **2**, 915-931.
2. J. F. Chang, L. G. Feng, C. P. Liu, W. Xing and X. L. Hu, *Angewandte Chemie-International Edition*, 2014, **53**, 122-126.
3. L. Y. Chen, H. Guo, T. Fujita, A. Hirata, W. Zhang, A. Inoue and M. W. Chen, *Adv. Funct. Mater.*, 2011, **21**, 4364-4370.
4. Z. Huang, Y. Liu, F. Y. Xie, Y. C. Fu, Y. He, M. Ma, Q. J. Xie and S. Z. Yao, *Chem. Commun.*, 2012, **48**, 12106-12108.
5. M. A. Matin, J. H. Jang and Y. U. Kwon, *J. Power Sources*, 2014, **262**, 356-363.
6. T. Maiyalagan, X. Wang and A. Manthiram, *Rsc Advances*, 2014, **4**, 4028-4033.
7. J. F. Zhang, Y. Xu and B. Zhang, *Chem. Commun.*, 2014, **50**, 13451-13453.

8. J. Yang, C. G. Tian, L. Wang and H. G. Fu, *J. Mater. Chem.*, 2011, **21**, 3384-3390.
9. S. Chakraborty and C. Retna Raj, *Carbon*, 2010, **48**, 3242-3249.
10. S. Zhang, Y. Y. Shao, G. P. Yin and Y. H. Lin, *Angewandte Chemie-International Edition*, 2010, **49**, 2211-2214.
11. V. Mazumder and S. Sun, *J. Am. Chem. Soc.*, 2009, **131**, 4588-4589.
12. L. L. Zhang, Y. W. Tang, J. C. Bao, T. H. Lu and C. Li, *J. Power Sources*, 2006, **162**, 177-179.
13. X. Chen, G. Wu, J. Chen, X. Chen, Z. Xie and X. Wang, *J. Am. Chem. Soc.*, 2011, **133**, 3693-3695.
14. H. Lee, S. E. Habas, G. A. Somorjai and P. Yang, *J. Am. Chem. Soc.*, 2008, **130**, 5406-5407.
15. N. V. Rees and R. G. Compton, *J. Solid State Electrochem.*, 2011, **15**, 2095-2100.
16. Y. Suo and I. M. Hsing, *Electrochim. Acta*, 2009, **55**, 210-217.
17. W. P. Zhou, A. Lewera, R. Larsen, R. I. Masel, P. S. Bagus and A. Wieckowski, *J. Phys. Chem. B*, 2006, **110**, 13393-13398.
18. C. Li, T. Sato and Y. Yamauchi, *Chem. Commun.*, 2014, **50**, 11753-11756.
19. X. Q. Huang, S. H. Tang, X. L. Mu, Y. Dai, G. X. Chen, Z. Y. Zhou, F. X. Ruan, Z. L. Yang and N. F. Zheng, *Nature Nanotechnology*, 2011, **6**, 28-32.
20. M. Jin, H. Zhang, Z. Xie and Y. Xia, *Energy & Environmental Science*, 2012, **5**, 6352-6357.
21. H. Meng, S. Sun, J. P. Masse and J. P. Dodelet, *Chem. Mater.*, 2008, **20**, 6998-7002.
22. Z. Cui, M. Yang and F. J. DiSalvo, *ACS Nano*, 2014, **8**, 6106-6113.
23. C. G. Hu, Y. Zhao, H. H. Cheng, Y. Hu, G. Q. Shi, L. M. Dai and L. T. Qu, *Chem. Commun.*, 2012, **48**, 11865-11867.
24. R. Ojani, Z. Abkar, E. Hasheminejad and J. B. Raoof, *Int. J. Hydrogen Energy*, 2014, **39**, 7788-7797.
25. S. E. Habas, H. Lee, V. Radmilovic, G. A. Somorjai and P. Yang, *Nat Mater*, 2007, **6**, 692-697.
26. A. N. Correia, L. H. Mascaro, S. A. S. Machado and L. A. Avaca, *Journal of the Brazilian Chemical Society*, 1999, **10**, 478-482.
27. R. S. Jayashree, J. S. Spendelow, J. Yeom, C. Rastogi, M. A. Shannon and P. J. A. Kenis, *Electrochim. Acta*, 2005, **50**, 4674-4682.
28. R. F. Wang, H. Wang, X. L. Wang, S. J. Liao, V. Linkov and S. Ji, *Int. J. Hydrogen Energy*, 2013, **38**, 13125-13131.
29. A. Ma, X. Zhang, X. Wang, L. Le and S. Lin, *RSC Advances*, 2015, **5**, 64534-64537.
30. S. Hu, L. Scudiero and S. Ha, *Electrochim. Acta*, 2012, **83**, 354-358.
31. K. C. Poon, D. C. L. Tan, T. D. T. Vo, B. Khezri, H. Su, R. D. Webster and H. Sato, *J. Am. Chem. Soc.*, 2014, **136**, 5217-5220.
32. A. Nassr, A. Quetschke, E. Koslowski and M. Bron, *Electrochim. Acta*, 2013, **102**, 202-211.
33. M. Zhao, K. Abe, S.-i. Yamaura, Y. Yamamoto and N. Asao, *Chem. Mater.*, 2014, **26**, 1056-1061.
34. Z. Liu, L. Hong, M. P. Tham, T. H. Lim and H. Jiang, *J. Power Sources*, 2006, **161**, 831-835.
35. J. Joo, T. Uchida, A. Cuesta, M. T. M. Koper and M. Osawa, *J. Am. Chem. Soc.*, 2013, **135**, 9991-9994.
36. J. Joo, T. Uchida, A. Cuesta, M. T. M. Koper and M. Osawa, *Electrochim. Acta*, 2014, **129**, 127-136.
37. S. Brimaud, J. Solla-Gullon, I. Weber, J. M. Feliu and R. J. Behm, *Chemelectrochem*, 2014, **1**, 1075-1083.
38. N. Arjona, M. Guerra-Balcazar, F. M. Cuevas-Muniz, L. Alvarez-Contreras, J. Ledesma-Garcia and L. G. Arriaga, *Rsc Advances*, 2013, **3**, 15727-15733.
39. M. H. Shao, J. Odell, M. Humbert, T. Y. Yu and Y. N. Xia, *Journal of Physical Chemistry C*, 2013, **117**, 4172-4180.
40. Y. Xia, J. Liu, W. Huang and Z. L. Li, *Electrochim. Acta*, 2012, **70**, 304-312.
41. Y. Wang, S.-I. Choi, X. Zhao, S. Xie, H.-C. Peng, M. Chi, C. Z. Huang and Y. Xia, *Adv. Funct. Mater.*, 2014, **24**, 131-139.
42. L. O. Gullman, *Journal of the Less Common Metals*, 1966, **11**, 157-167.